Detection of the Askja AD 1875 cryptotephra in Latvia, Eastern Europe

Normunds Stivrins[1,2,3]*, Sabine Wulf[4,5,6], Stefan Wastegård[7], Ewa M Lind[7], Tiiu Alliksaar[2], Mariusz Gałka[8], Thorbjørn Joest Andersen[9], Atko Heinsalu[2], Heikki Seppä[1], Siim Veski[2]

[1]Department of Geosciences and Geography, University of Helsinki, P.O. Box 64, FI-00014, Helsinki, Finland
[2]Institute of Geology, Tallinn University of Technology, Ehitajate tee 5, 19086, Tallinn, Estonia
[3]Lake and Peatland Research Centre, Puikule, LV-4063, Latvia
[4]Senckenberg Research Institute and Natural History Museum, BIK-F, TSP6 Evolution and Climate, Senckenberganlage 25, D-60325 Frankfurt A.M., Germany
[5]GFZ German Research Centre for Geosciences, Section – 5.2 Climate Dynamics and Landscape Evolution, Telegrafengerg, 14473, Potsdam, Germany
[6]Institute for Geosciences, Heidelberg University, Im Neuenheimer Feld 234, D-69120 Heidelberg, Germany
[7]Department of Physical Geography, Stockholm University, SE-106 91, Stockholm, Sweden
[8]Department of Biogeography and Palaeoecology, Faculty of Geographical and Geological Sciences, Adam Mickiewicz University, Dziegielowa 27, 61-680, Poznan, Poland
[9]Department of Geosciences and Natural Resource Management, University of Copenhagen, Oester Voldgade 10, 1350 Copenhagen K, Denmark

* Corresponding author, E-mail: normunds.stivrins@helsinki.fi (N. Stivrins)

ABSTRACT

We report the first geochemically confirmed findings of the Askja volcano (Iceland) AD 1875 eruption cryptotephra in Eastern Europe. The cryptotephra finding in Latvia is the easternmost finding of the Askja AD 1875 so far, providing an important time marker in the sediments. Even though low concentrations of Askja AD 1875 rhyolitic

glass shards were recorded, our findings suggest the possibilities of also tracing other historical cryptotephras in lacustrine and peat sediments in Eastern Europe. We use the Askja AD 1875 tephra isochrone to synchronize pollen data of human activities, i.e. the rye (*Secale cereale*) cultivation. Our comparison of *Secale* pollen from two sites reveals that there were minor dissimilarities in the timing of highest rye cultivation, and that synchronous decrease of rye cultivation occurred at both sites few years after the Askja eruption at AD 1875.

KEYWORDS: Askja AD 1875; tephrochronology; cryptotephra; EMPA; Latvia.

Introduction

The Askja AD 1875 eruption was the largest Plinian eruption in Iceland during the historical times, dispersing volcanic ash (tephra) over wide areas in northern Europe (e.g. Mohn, 1878; Carey *et al*., 2010). Beside numerous tephra findings in Northern Europe (e.g. Persson, 1971; Oldfield *et al*., 1997; Boygle, 1998; van den Bogaard and Schmincke, 2002; Bergman *et al*., 2004; Pilcher *et al*., 2005; Wastegård, 2005; Davies *et al*., 2007; Wastegård and Davies, 2009), cryptotephra of the Askja AD 1875 eruption has recently also been detected in northeastern Germany and northern Poland (Tylmann *et al*., 2016; Wulf *et al*., 2016).

The total volume estimates for the Askja AD 1875 eruption revealed a mass discharge as large as 1.37 km^3, which is of comparable size to the volcanic eruption of Mount St. Helens in AD 1980 (Carey *et al*., 2010). In comparison, the recent small-to-intermediate size eruption of the Icelandic volcano Eyjafjallajökull in April 2010 produced approximately 0.27 km^3 of airborne tephra that dispersed over Europe and the North Atlantic and led to a global disruption of air travel (Davies *et al*., 2010; Gudmundsson *et al*., 2012). Jensen *et al*. (2014) showed that cryptotephra of such moderate-size eruptions can have substantially larger distributions than previously assumed. This highlights the vulnerability of modern human society to such natural hazards, even during modest eruptions. Thus, reconstructions of past eruption plume envelopes help evaluate future potential volcanic hazards (e.g. Thordarson and Self, 2003; Riede and Bazely, 2009; Capra *et al*., 2014; Dellino *et al*., 2014; Oppenheimer, 2015; Ponomareva *et al*., 2015). The development and advances in tephrochronology (Dugmore, 1989; Turney, 1998; Lowe, 2011), greatly contributed to the finding of even

tiny amounts of dispersed ash (cryptotephra) in distal and ultra-distal locations and thus to the improvement of tephra dispersal maps. Tephrochronology is used in palaeoenvironmental records in terrestrial-lacustrine and marine settings in order to synchronise records and provide precise time and synchronisation markers (e.g. Lowe, 2011; Lane *et al*., 2013; Wulf *et al*., 2013; Brauer *et al*., 2014; Davies, 2015; Wulf *et al*., 2016).

In this study, we present a new discovery of the historic Askja AD 1875 cryptotephra in three sites in Latvia, Eastern Europe. We apply the tephrochronological results of two lake sequences (Lake Āraišu, Lake Trikātas) and one peat record (Teiči Bog) to: (1) extend the modelled (Carey *et al*., 2010) dispersal fan of the Askja AD 1875 tephra further to the east and (2) demonstrate how this cryptotephra can be used for synchronisation of rye pollen (*Secale cereale*) curves. Rye was selected here because it was an important agricultural and economical staple. Hence, precise chronology may improve historical and paleoecological knowledge on importance and dynamics of rye abundance.

Study sites and background information

Two lacustrine sediment sequences and one peat core in eastern, central and northern Latvia were collected for tephrochronological studies (Figure 1).

Lake Āraišu (57°15'N, 25°17'E, 120.2 m a.s.l.) is located in central Latvia and has a surface area of 32.6 ha. Lake Trikātas (57°32'N, 25°42'E, 50 m a.s.l.) is situated in northern Latvia, and the surface area covers 13 ha. Both lakes were sampled with a 1 m-long Russian peat sampler at the deepest point of the lake (12.3 m at Lake Āraišu and 4 m at Lake Trikātas) through ice in 2012 and 2013, respectively. The topmost 0.5 m of unconsolidated sediment was sampled using a Willner-type gravity sampler. Lake Āraišu revealed a 12.4 m-long sediment sequence of homogeneous gyttja (Stivrins *et al*., 2015), while a 8 m-long sequence of alternating silt and homogeneous gyttja was obtained from Lake Trikātas (Stivrins *et al*., 2016). Both sequences were analysed for pollen, non-pollen palynomorphs, loss-on-ignition and magnetic susceptibility (Stivrins *et al*., 2015; 2016).

Teiči Bog (56°37'N, 26°26'E, 108.5 to 114 m a.s.l.) is located in eastern Latvia and covers an area of ca. 14,400 ha. Sampling of the uppermost meter of the peat deposits occurred in August 2013 at the dome of Teiči Bog using a Wardenaar corer.

Chronology

The sediment chronology of Lake Āraišu is based on 12 bulk ^{14}C dates and spheroidal carbonaceous particles (SCP). The peak in SCP emissions occurred in AD 1982±10 (Latvenergo electric utility company emissions data; Stivrins *et al*., 2015). The age model of the Lake Trikātas sediment sequence was established by six AMS ^{14}C dates (Stivrins *et al*., 2016). The chronology of Teiči Bog peat is based on radionuclide dating of ^{210}Pb,^{137}Cs and ^{241}Am, SCP and 11 accelerator mass spectrometry (AMS) ^{14}C samples of *Sphagnum* stems (Supporting Information 1–2). Radioactive isotope concentrations were measured at the Gamma Dating Centre Copenhagen, University of Copenhagen, Denmark. Conventional ^{14}C dating was processed at the Institute of Geology, Tallinn University of Technology, Estonia (Tln), and AMS ^{14}C samples were measured at the Poznan Radiocarbon Laboratory, Poland (Poz) and the Scottish Universities Environmental Research Centre, United Kingdom (GU).

Since the Bayesian approach provides more robust estimates of uncertainty than the classical approach using linear or spline modes, an age-depth model of each sequence (Figure 2) was produced using Bacon 2.2 (Blaauw and Christen, 2011). Bacon 2.2 divides a core into a large number of thin vertical sections, and models the accumulation rate of each section (Blaauw and Mauquoy, 2012). We used function *pMC.age* to calculate radiocarbon ages for post-bomb dates. Individual ^{14}C calibration was carried out by using the IntCal13 calibration dataset (Reimer *et al*., 2013) with a 2σ (95.4%) confidence level. All age modelling was performed in the R environment (version 3.0.3) (R Core Team, 2014).

Tephrochronological methods

Lake and peat sediments were sampled in 1-cm (Lake Āraišu: 1290-1296 cm depth; Lake Trikātas: 450-465 cm depth) and 2-cm increments (Teiči Bog: 58-66 cm depth) in sections of the considered time frame of the Askja AD 1875 eruption and processed for glass shard extraction. In order to remove organic matter fresh peat samples from Teiči Bog were combusted at 550°C for 4 hours, while sediments from lakes Āraišu and Trikātas were treated with a 15% hydrogen peroxide solution overnight. All sediments were processed with a 10% hydrochloric acid solution in order to dissolve carbonates. Samples were subsequently wet-sieved into a 20-100 µm grain size fraction

and dried with ethanol. Glass shards of the 20-100 µm fraction were handpicked under a transmitted light microscope into a single-hole stub, embedded in Araldite©2020 resin, sectioned and polished manually on silicon carbide paper, and finally carbon coated for electron probe microanalyses (EPMA). The major element composition of single glass shards was determined on a JEOL-JXA8230 instrument at the GFZ Potsdam using a 15 kV voltage, a 10 nA beam current and a beam size of 5 µm (Lake Āraišu, Teiči Bog) and 8 µm (Lake Trikātas). Exposure time was 20 seconds for Fe, Cl, Mn, Ti, Mg and P, and 10 seconds for F, Si, Al, K, Ca and Na. Instrumental calibration used natural minerals and the rhyolitic Lipari obsidian glass standard (Hunt and Hill, 1996; Kuehn *et al*., 2011). Major element raw data and standard analysis data are listed in Supporting Information 3 and compared as normalised (volatile-free) data to published EPMA glass data of potential tephra correlatives (Figure 3).

Results

Tephra identification

Relatively low numbers of highly vesicular, colourless to light brownish glass shards were detected at all three sites in one respective single peak sample (Figure 2). Important to note that the cryptotephra isochrones improved previous age-model estimates for both Lake Trikātas and Āraišu, particularly for the uppermost sediment sections. No shards have been found in the sediment samples above or below those peak samples. Lake Āraišu and Lake Trikātas sediments exhibited a total of 12 shards cm^{-3} and eight shards cm^{-3} at 1293-1294 cm and at 457-458 cm depth (below lake water surface), respectively. All shards were geochemically characterised (Supporting Information 3). More than 45 glass shards were identified in the 2-cm^3 – sample of Teiči Bog at the depth of 60-62 cm, of which seven shards were analysed (Supporting Information 3). Glass shards of all samples show a similar rhyolitic composition to Icelandic provenance with SiO_2 concentration ranges of 71.6-76.1 wt% and Al_2O_3 of 12.0-13.2 wt% (normalized data). Glass shards from Lake Āraišu reveal slightly higher SiO_2 and lower Al_2O_3 and Na_2O concentrations (Figure 3) indicating sodium migration likely due to the use of a small beam size of 5 µm during EPMA analyses. According to the bivariate plots, the glass compositions of all three samples from Latvia correlates best to the Askja AD 1875 tephra and are distinct from other historical Icelandic silicic tephras by lower K_2O contents (2.1-2.7 wt%) (Figure 3). Also the high MgO is typical

for Askja AD 1875 tephra (e.g. Sigurdsson and Sparks, 1981; Larsen *et al*., 1999) and separates it from most other rhyolitic tephras from Iceland.

Discussion and conclusions

Usefulness for dating historical palaeoenvironmental records

We report the first discovery of the Askja AD 1875 cryptotephra east of the longitude 25ºE in Eastern Europe. The identification in Latvia is the easternmost finding of this cryptotephra so far, providing an important time marker in sediments at AD 1875. Even though low concentrations of Askja AD 1875 rhyolitic glass shards were recorded, our findings suggest the possibilities for tracing other historical cryptotephra isochrones in both lacustrine and peat sediments in Eastern Europe. Utilisation of historical cryptotephra may serve as an important tool not only in palaeoenvironmental studies but also in archaeology (e.g. Housley *et al*., 2015). Furthermore, natural and artificial atmospheric fall-out radionuclides, such as ^{210}Pb and ^{137}Cs, are commonly used to date recent sediment and peat deposits (up to the last 150 a). However, the half-life of ^{210}Pb is 22.3 years, and after 5–7 half-lives the amount of ^{210}Pb activity in a samples becomes statistically undetectable (Le Roux and Marshall, 2011). Consequently, Askja AD 1875 and potentially other historical cryptotephras from Iceland (e.g. Landnám AD 870s, Öræfajökull AD 1362, Hekla AD 1947) may become more valuable isochrones as stratigraphic markers in Eastern Europe. Moreover, tentative finding of middle Holocene cryptotephra (Hekla-4 eruption) from western Estonia (Hang *et al*., 2006) indicates that eastwards cryptotephra records might be more widespread.

Synchronisation of palaeoenvironmental records

Using the Askja AD 1875 tephra as an isochrone, it is possible to improve chronologies and compare data of human activities such as the history of rye (*Secale cereale*) cultivation at Lake Āraišu (Stivrins *et al*., 2015) and Lake Trikātas (Stivrins *et al*., 2016). Based on the pollen data, intensive rye cultivation has been practiced at Lake Āraišu since AD 700, with the peak at AD 1880 (Figure 4). At Lake Trikātas rye was sever cultivated since AD 1200 with a peak at AD 1800. Increases in *Secale* pollen do not automatically imply an increase in the amount of rye cultivation, but instead may reflect a more efficient use of existing agricultural land achieved through intensification and modernisation of arable farming techniques (Stivrins *et al*., 2016). Our comparison

199 reveals that it is possible to distinguish not only minor dissimilarities in the timing of
200 rye cultivation intensification, but also that synchronous decrease of *Secale* pollen at
201 both locations took place few years after AD 1875 (Figure 4). This can possibly be
202 related to the changes in land ownership, land-use management (from arable land to
203 pasture and meadow), the beginning of potato (*Solanum tuberosum*) cultivation as well
204 as the end of the 'golden era' of rye-based spirit production in the Baltic lands of the
205 Russian Empire (Niinemets and Saarse, 2009; Stivrins *et al*., 2016). Likewise, the
206 reduction of land-use area and subsequent decrease in rye cultivation can be a result of
207 change from a subsistence extensive farming system to a more intensive farming
208 economy due to increased crop yields in the Baltic area (Veski *et al*., 2005).
209
210 *Acknowledgements*

211 We would like to thank Oona Appelt from the GFZ Potsdam for help with electron
212 probe microanalyses of tephra shards. Research was supported by the project EBOR,
213 IUT 1-8 and the Latvian Peat Producer's Association. We acknowledge support for this
214 study from the INTIMATE EU COST Action in the form of a Short-Term Scientific
215 Mission.
216

217 ## References

218 Andersson S, Rosqvist G, Leng MJ, Wastegård S, Blaauw M. 2010. Late Holocene
219 climate change in central Sweden inferred from lacustrine stable isotope data.
220 *Journal of Quaternary Science* **25**: 1305-1316.
221 Bergman J, Wastegård S, Hammarlund D, Wohlfarth B, Roberts SJ. 2004. Holocene
222 tephra horizons at Klocka Bog, west-central Sweden: aspects of reproducibility
223 in subarctic peat deposits. *Journal of Quaternary Science* **19**: 241–249.
224 Blaauw M, Christen JA. 2011. Flexible paleoclimate age-depth models using an auto-
225 regressive gamma process. *Bayesian Analysis* **6**: 457–474.
226 Blaauw M, Mauquoy D. 2012. Signal and variability within a Holocene peat bog -
227 Chronological uncertainties of pollen, macrofossil and fungal proxies. *Review of*
228 *Palaeobotany and Palynology* **186**: 5–15.
229 Boygle J. 1998. A little goes a long way: discovery of a new mid-Holocene tephra in
230 Sweden. *Boreas* **27**: 195–199.

231 Brauer A, Hajdas I, Blockley SPE, Bronk Ramsey C, Christl M, Ivy-Ochs S, Moseley
232 GE, Nowaczyk NN, Rasmussen SO, Roberts HM, Spötl C, Staff RA, Svensson
233 A. 2014. The importance of independent chronology in integrating records of past
234 climate change for the 60–8 ka INTIMATE time interval. *Quaternary Science*
235 *Reviews* **106**: 47–66.
236 Capra L, Gavilanes-Ruiz JC, Bonasia R, Saucedo-Giron R, Sulpizio R. 2014. Re-
237 assessing volcanic hazard zonation of Volcán de Colima, México. *Natural*
238 *Hazards* **76**: 41–61.
239 Carey RJ, Houghton BF, Thordarson T. 2010. Tephra dispersal and eruption dynamics
240 of wet and dry phases of the 1875 eruption of Askja Volcano, Iceland. *Bulletin of*
241 *Volcanology* **48**: 109–125.
242 Davies SM, Elmquist M, Bergman J, Wohlfarth B, Hammarlund D. 2007. Cryptotephra
243 sedimentation processes within two lacustrine sequences from west central
244 Sweden. *The Holocene* **17**: 1–13.
245 Davies SM, Larsen G, Wastegård S, Turney CSM, Hall VA, Coyle L, Thordarson T.
246 2010. Widespread dispersal of Icelandic tephra: how does the Eyjafjöll eruption
247 of 2010 compare to past Icelandic events? *Journal of Quaternary Science* **25**:
248 605–611.
249 Davies SM. 2015. Cryptotephras: the revolution in correlation and precision dating.
250 *Journal of Quaternary Science* **30**: 114–130.
251 Dellino P, Dioguardi F, Mele D, D'Addabbo M, Zimanowski B, Büttner R, Doronzo
252 DM, Sonder I, Sulpizio R, Dürig T, La Volpe L. 2014. Volcanic jets, plumes, and
253 collapsing fountains: evidence from large-scale experiments, with particular
254 emphasis on the entrainment rate. *Bulletin of Volcanology* **76**: 834–852.
255 Dugmore AJ. 1989. Icelandic volcanic ash in late-Holocene peats in Scotland. *Scottish*
256 *Geographical Magazine* **105**: 169–172.
257 Gudmundsson MT, Thordarson T, Höskuldsson Á, Larsen G, Björnsson H, Prata F,
258 Oddsson B, Magnússon E, Högnadóttir T, Petersen GN, Hayward CL, Stevenson
259 JA, Jónsdóttir I. 2012. Ash generation and distribution from the April-May 2010
260 eruption of Eyjafjallajökull, Iceland. *Scientific Reports* **2**: 572–584.
261 Hang T, Wastegård S, Veski S, Heinsalu A. 2006. First discovery of cryptotephra in
262 Holocene peat deposits of Estonia, eastern Baltic. *Boreas* **35:** 644–649.

263 Housley RA, Gamble CS, RESET Associates. 2015. Examination of Late Palaeolithic
264 archaeological sites in northern Europe for the preservation of cryptotephra
265 layers. *Quaternary Science Reviews* **118**: 142–150.
266 Hunt JB, Hill PG. 1996. An inter-laboratory comparison of the electron probe
267 microanalysis of glass geochemistry. *Quaternary International* **34-36**: 229–241.
268 Jensen BJL, Pyne-O'Donnell S, Plunkett G, Froese DG, Hughes PDM, Sigl M,
269 McConnell JR, Amesbury MJ, Blackwell PG, van den Bogaard C, Buck CE,
270 Charman DJ, Clague JJ, Hall VA, Koch J, Mackay H, Mallon G, McColl L,
271 Pilcher JR. 2014. Transatlantic distribution of the Alaskan White River Ash.
272 *Geology* **42**: 875–878.
273 Kuehn SC, Froese DG, Shane PAR, INTAV Intercomparison Participants. 2011. The
274 INTAV intercomparison of electron-beam microanalysis of glass by
275 tephrochronology laboratories: Results and recommendations. *Quaternary*
276 *International* **246**: 19–47.
277 Lane CS, Brauer A, Blockley SPE, Dulski P. 2013. Volcanic ash reveals time-
278 transgressive abrupt climate change during the Younger Dryas. *Geology* **41**:
279 1251–1254.
280 Larsen G, Dugmore A, Newton AJ. 1999. Geochemistry of historical-age silicic tephras
281 in Iceland. *The Holocene* **9**: 463-471.
282 Le Roux G, Marshall WA. 2011. Constructing recent peat accumulation chronologies
283 using atmospheric fall-out radionuclides. *Mires and Peat* **7**: 1–14.
284 Lowe DJ. 2011. Tephrochronology and its application: A review. *Quaternary*
285 *Geochronology* **6**: 107–153.
286 Mohn H. 1878. Askeregnen den 29de–30te Marts 1875 (The tephra fall on 29–30 March
287 1875). *Forhandlinger I Videnskapsselskabet I Christiania aar 1877* **10**: 1-12.
288 Niinemets E, Saarse L. 2009. Holocene vegetation and land-use dynamics of south-
289 eastern Estonia. *Quaternary International* **207**: 104–116.
290 Oldfield F, Thompson R, Crooks PRJ, Gedye SJ, Hall VA, Harkness DD, Housley RA,
291 McCormac FG, Newton AJ, Pilcher JR, Renberg I, Richardson N. 1997.
292 Radiocarbon dating of a recent high latitude peat profile: Stor Amyran, northern
293 Sweden. *The Holocene* **7**: 283–290.
294 Oppenheimer C. 2015. Eruption politics. *Nature Geoscience* **8**: 244–245.
295 Persson C. 1971. Tephrachronological investigation of peat deposits in Scandinavia and
296 on the Faeroe Islands. Sveriges Geologiska Undersoknin 65: 1–34.

297 Pilcher JR, Bradley RS, Francus P, Anderson L. 2005. A Holocene tephra record from
298 the Lofoten Islands, Arctic Norway. *Boreas* **34**: 136–156.
299 Ponomareva V, Portnyagin M, Davies SM. 2015. Tephra without Borders: Far-
300 Reaching Clues into Past Explosive Eruptions. *Frontiers in Earth Science* **3**: 1–
301 16.
302 R Core Team. 2014. R: A language and environment for statistical computing. R
303 Foundation for Statistical Computing, Vienna. URL http://www.R-project.org/
304 Reimer PJ, Bard E, Bayliss A, Beck JW, Blackwell PG, Bronk Ramsey C, Buck CE,
305 Cheng H, Edwards RL, Friedrich M, Grootes PM, Guilderson TP, Haflidason H,
306 Hajdas I, Hatté C, Heaton TJ, Hoffmann DL, Hogg AG, Hughen KA, Kaiser KF,
307 Kromer B, Manning SW, Niu M, Reimer RW, Richards DA, Scott EM, Southon
308 JR, Staff RA, Turney CSM, van der Plicht J. 2013. IntCal13 and Marine13
309 radiocarbon age calibration curves, 0-50,000 years cal BP. *Radiocarbon* **55**:
310 1869–1887.
311 Riede F, Bazely O. 2009. Testing the 'Laacher See hypothesis': a health hazard
312 perspective. *Journal of Archaeological Science* **36**: 675–683.
313 Sigurdsson H, Sparks RSJ. 1981. Petrology of rhyolitic and mixed magma ejecta from
314 the 1875 eruption of Askja, Iceland. *Journal of Petrology* **22**: 41-84.
315 Stivrins N, Brown A Reitalu T, Veski S, Heinsalu A, Banerjea RY, Elmi K. 2015.
316 Landscape change in central Latvia since the Iron Age: multi-proxy analysis of
317 the vegetation impact of conflict, colonization and economic expansion during
318 the last 2,000 years. *Vegetation History and Archaeobotany* **24**: 377–391.
319 Stivrins N, Brown A, Veski S, Ratniece V, Heinsalu A, Austin J, Liiv M, Ceriņa A.
320 2016. Palaeoenvironmental evidence for the impact of the crusades on the local
321 and regional environment of medieval (13^{th}-16^{th} century) northern Latvia, eastern
322 Baltic. *The Holocene* **26**: 61–69.
323 Thordarson T, Self S. 2003. Atmospheric and environmental effects of the 1783-1784
324 Laki eruption: A review and reassessment. *Journal of Geophysical Research:*
325 *Atmospheres* **108 (D1)**: 40111.
326 Turney CSM. 1998. Extraction of rhyolitic component of Vedde microtephra from
327 minerogenic lake sediments. *Journal of Paleolimnology* **19**: 199–206.
328 Tylmann W, Bonk A, Goslar T, Wulf S, Grosjean M. 2016. Calibrating ^{210}Pb dating
329 results with varve chronology and independent chronostratigraphic markers:
330 problems and implications. *Quaternary Geochronology* **32**: 1–10.

van den Bogaard C, Schmincke H-U. 2002. Linking the North Atlantic to central Europe: a high-resolution Holocene tephrochronological record from northern Germany. *Journal of Quaternary Science* **17**: 3–20.

Veski S, Koppel K, Poska A. 2005. Integrated palaeoecological and historical data in the service of fine-resolution land use and ecological change assessment during the last 1000 years in Rõuge, southern Estonia. *Journal of Biogeography* **32**: 1473–1488.

Wastegård S, Davies SM. 2009. An overview of distal tephrochronology in northern Europe during the last 1000 years. *Journal of Quaternary Science* **24**: 500–512.

Wastegård S. 2005. Late Quaternary tephrochronology of Sweden: a review. *Quaternary International* **130**: 49–62.

Wulf S, Dräger N, Ott F, Serb J, Appelt O, Guðmundsdóttir E, van den Bogaard C, Słowiński M, Błaszkiewicz M, Brauer A. 2016. Holocene tephrostratigraphy of varved sediment records from Lakes Tiefer See (NE Germany) and Czechowskie (N Poland). *Quaternary Science Reviews* **132**: 1-14.

Wulf S, Ott F, Slowinski M, Noryskiewicz AM, Dräger N, Martin-Puertas C, Czymzik M, Neugebauer I, Dulski P, Bourne AJ, Blaszkiewicz M, Brauer A. 2013. Tracing the Laacher See Tephra in the varved sediment record of the Trzechowskie palaeolake in central Northern Poland. *Quaternary Science Reviews* **76**: 129–139.

365 **Figure and Supporting Information captions**

366

367

368

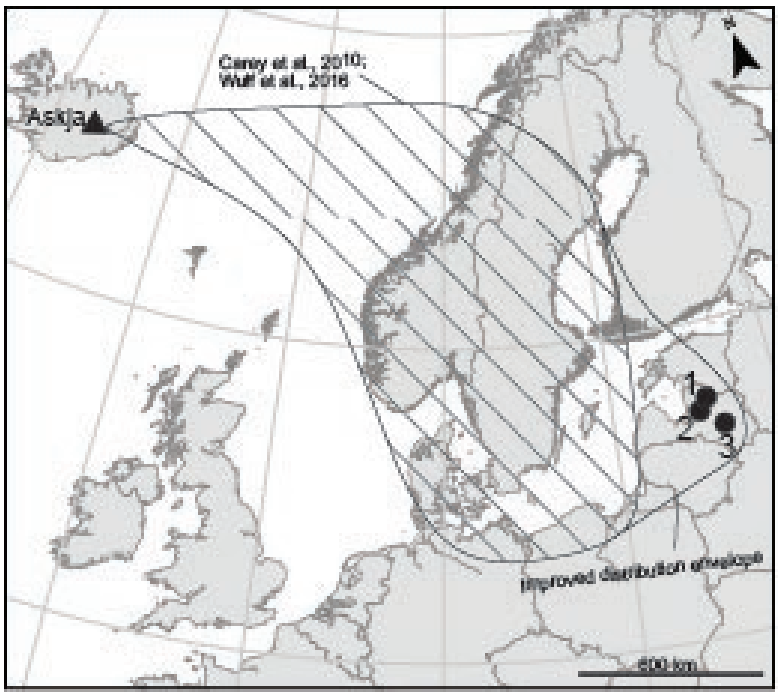

369

370

371 **Figure 1.** Location of study sites in Latvia, with the currently known detected limit of
372 dispersal envelope of Askja AD 1875 (Carey *et al*., 2010; Wulf *et al*., 2016) and
373 improved distribution envelope. 1=Lake Trikātas; 2= Lake Āraišu; 3= Teiči Bog.

374

375

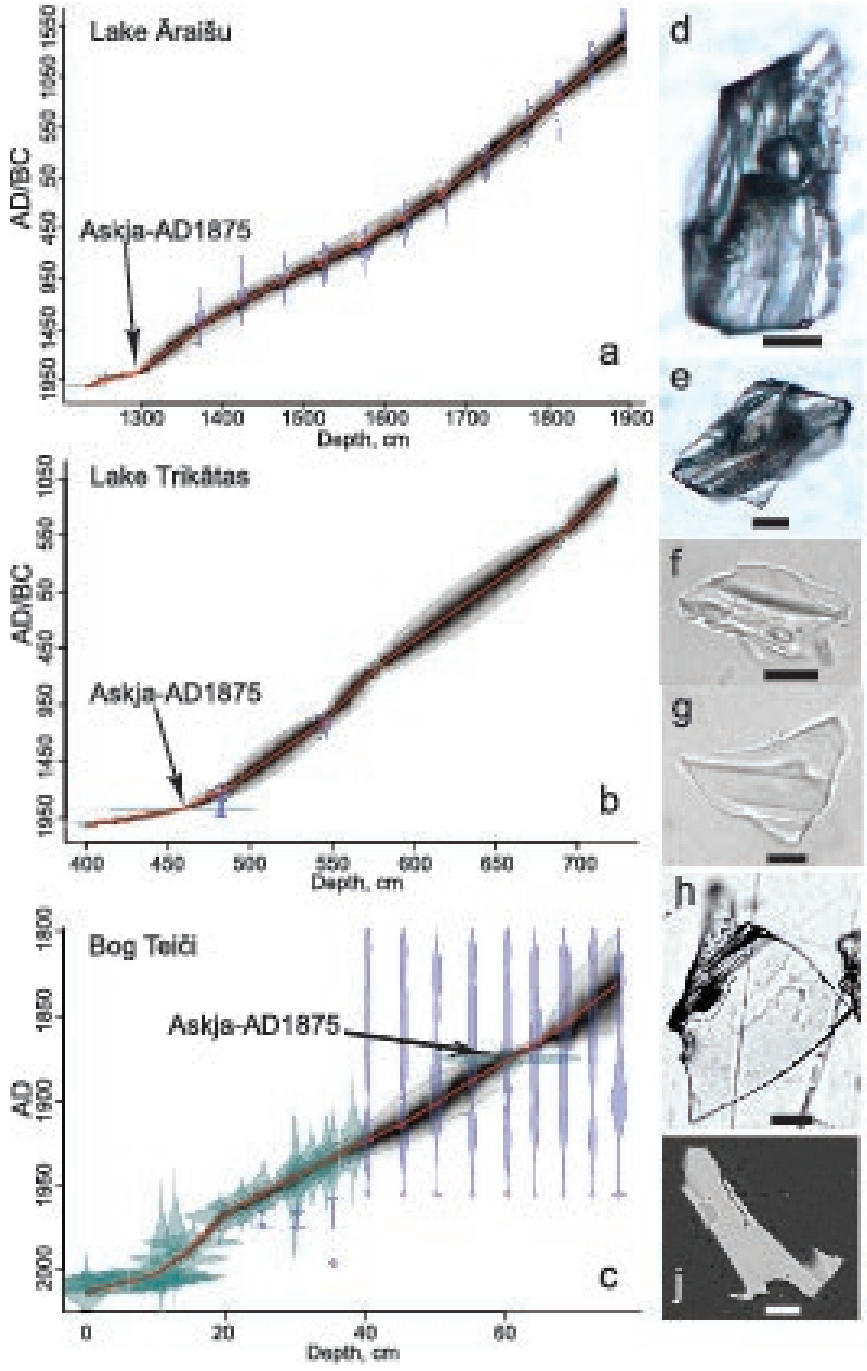

Figure 2. Age-depth model of (a) Lake Āraišu, (b) Lake Trikātas and (c) Teiči Bog. Age-depth model based on ^{14}C (purple) and ^{210}Pb, spheroidal carbonaceous particles and cryptotephra of Askja AD 1875 (turquoise) dates. The red curve shows the weighted mean ages of all depths, whereas greyscales show uncertainties (where darker grey indicates more certain section). Selection of images of glass shards from the Askja AD 1875 tephra identified in the Latvian sites (this study): d–j scale bar 10 µm. Transmitted light images of tephra glass shards from binocular (d-h) and polarizing microscope (j). The figure is available in colour at online version of this article.

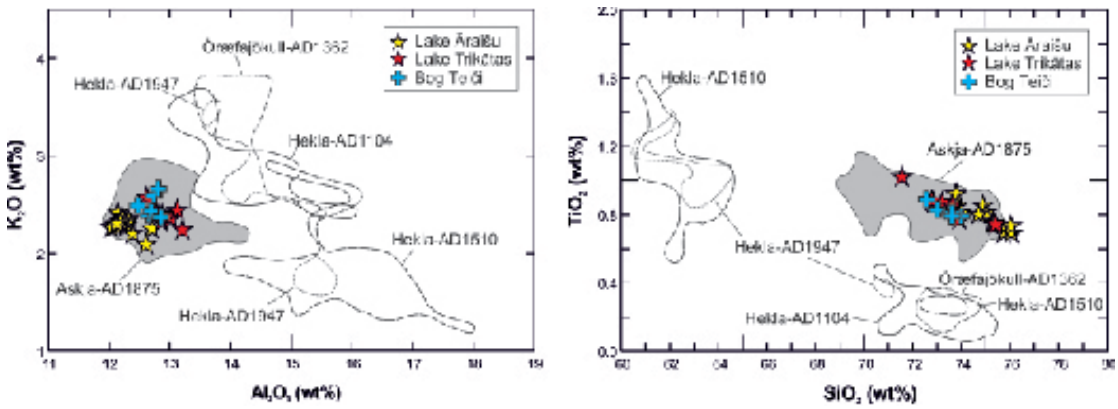

Figure 3. Chemical bi-plots for discriminating tephra found in Lake Āraišu (yellow stars), Lake Trikātas (red stars) and Teiči Bog (blue crosses) from major historical Icelandic eruptions presented as K_2O wt% vs. Al_2O_3 wt% and TiO_2 wt% vs. SiO_2 wt%. Comparing EPMA glass data are obtained from (1) Larsen *et al*. (1999) and (2) Andersson *et al*. (2010), Bergman *et al*. (2004), Boygle (1998), Oldfield *et al*. (1997), Pilcher *et al*. (2005), Sigurdsson and Sparks (1981), van den Bogaard and Schmincke (2002), and Wulf *et al*. (2016). The figure is available in colour at online version of this article.

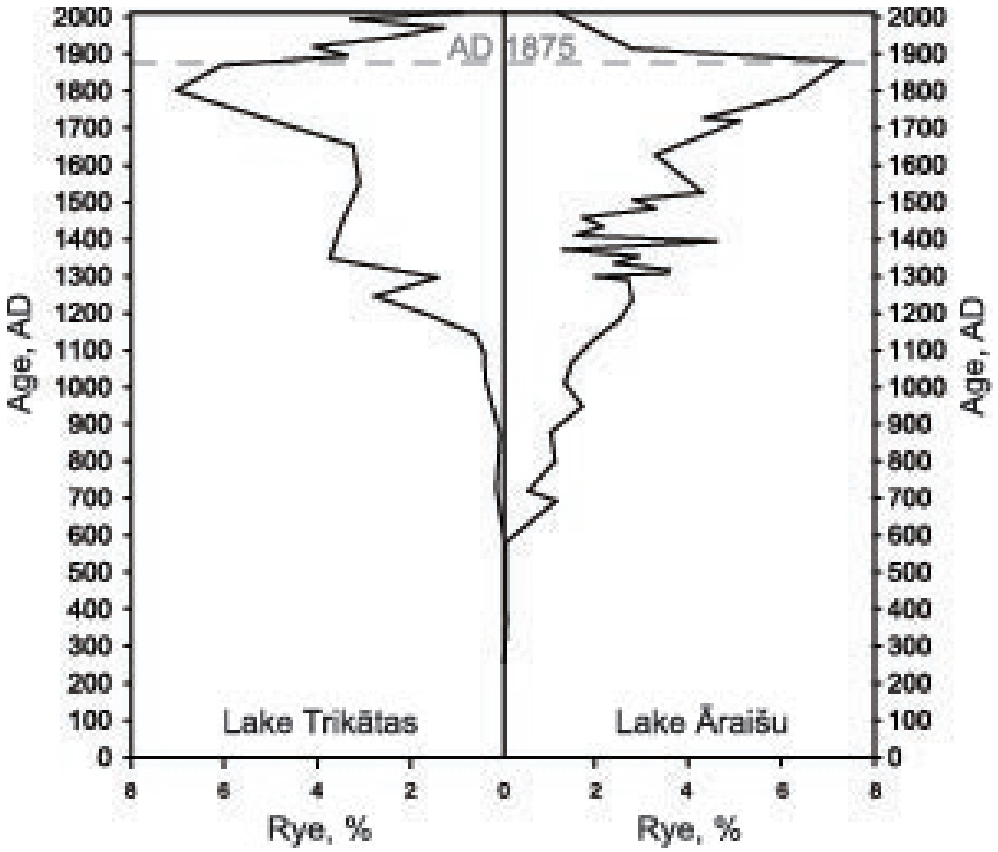

Figure 4. Synchronized rye (*Secale cereale*) pollen (%) of the last 2000 years for Lake Āraišu (Stivrins *et al*., 2015) and Trikātas (Stivrins *et al*., 2016).

Supporting Information 1. Teiči Bog AMS ^{14}C dates.

Supporting Information 2. Radionuclide dating and measurement results of Teiči Bog.

Supporting Information 3. Individual major-element glass data of the Askja AD 1875 tephra in Lake Āraišu, Lake Trikātas and Teiči Bog, and the Lipari obsidian standard glass beam size obtained by electron probe

Supporting Information 1. Teiči Bog AMS ^{14}C dates.

Depth, cm	Lab. no.	Age ^{14}C	Cal. a 95% ranges	Material dated
25–26	Poz-58406	144.61±0.4 pMC	-2963±22 BP	*Sphagnum* stems
30–31	Poz-58407	143.98±0.38 pMC	-2928±21 BP	*Sphagnum* stems
35–36	Poz-58408	111.44±0.31 pMC	-870±22 BP	*Sphagnum* stems
40–41	Poz-58409	135±25 BP	1800–1890 AD	*Sphagnum* stems
45–46	Poz-58411	125±25 BP	1800–1895 AD	*Sphagnum* stems
50–51	Poz-58412	80±25 BP	1810–1920 AD	*Sphagnum* stems
55–56	Poz-58413	120±25 BP	1800–1940 AD	*Sphagnum* stems
60–61	Poz-58414	125±25 BP	1800–1895 AD	*Sphagnum* stems
64–65	Poz-58415	100±25 BP	1810–1930 AD	*Sphagnum* stems
68–69	Poz-58416	100±30 BP	1805–1935 AD	*Sphagnum* stems
72–73	Poz-58417	125±25 BP	1800–1895 AD	*Sphagnum* stems

Supporting Information 2. Radionuclide dating and measurement results of Teiči Bog

Depth, cm	Age, a	Error age, a	Date, a
1.5	2	1	2011 AD
3.5	4	1	2009 AD
5.5	6	1	2007 AD
7.5	8	1	2005 AD
8.5	9	1	2004 AD
9.5	10	1	2003 AD
10.5	12	2	2001 AD
13.5	20	2	1993 AD
15.5	30	2	1983 AD
19.5	45	3	1968 AD
22.5	52	3	1961 AD
25.5	59	4	1954 AD
30.5	70	5	1943 AD
32.5	74	6	1939 AD
34.5	77	6	1936 AD
35.5	79	6	1934 AD
38.5	89	9	1924 AD

Depth	Pb-210tot	error Pb-210 tot	Pb-210 sup
cm	Bq kg-1	Bq kg-1	Bq kg-1
1.5	376	52	13
3.5	479	56	0
5.5	691	64	3
7.5	459	33	9
8.5	445	40	0
9.5	419	48	0
10.5	527	55	8
13.5	481	37	0
15.5	447	39	0
19.5	233	32	0
22.5	161	21	5
25.5	149	21	0
30.5	112	17	3
32.5	52	9	4
34.5	72	12	0
35.5	77	11	4
38.5	92	15	9

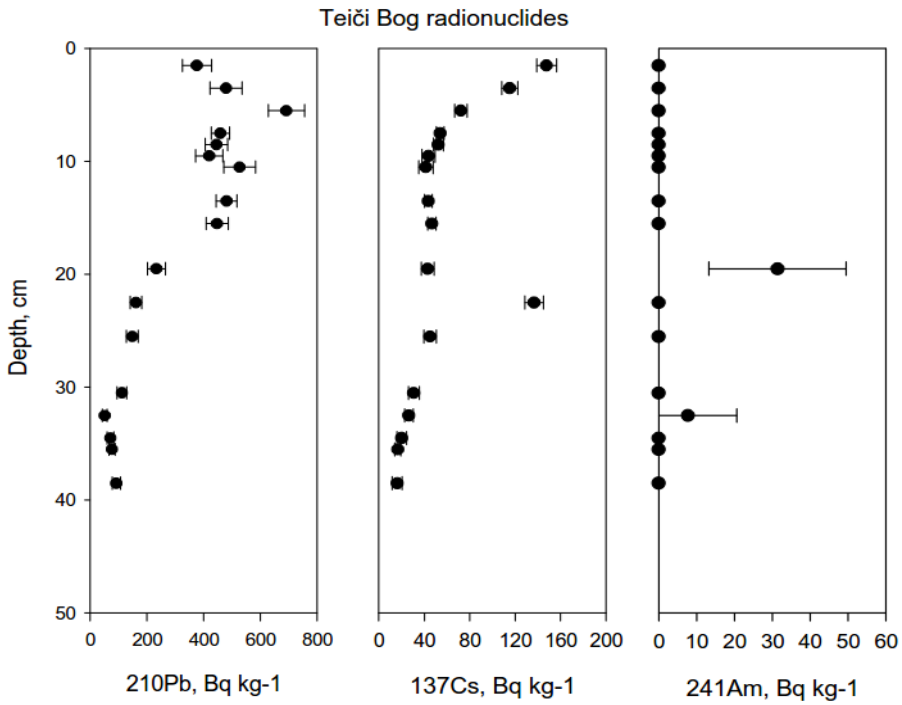

error Pb-210 sup	Pb-210 unsup	error Pb-210 unsup	Cs-137	error Cs-137	Am-241	error Am-241
Bq kg-1	Bq kg-1	Bq kg-1	Bq kg-1	Bq kg-1	Bq kg-1	Bq kg-1
10	363	52	148	9	0	0
0	479	56	115	7	0	0
4	688	64	72	5	0	0
2	450	33	54	3	0	0
0	445	40	52	4	0	0
0	419	48	44	6	0	0
15	518	57	41	6	0	0
0	481	37	44	4	0	0
0	447	39	47	4	0	0
0	233	32	43	6	31	18
1	156	21	137	8	0	0
0	149	21	45	6	0	0
6	109	18	31	5	0	0
7	48	11	26	4	8	13
0	72	12	20	4	0	0
7	74	13	17	3	0	0
1	84	15	16	4	0	0

Supporting Information 3. Individual major-element glass data of the Askja AD 1875 tephra in Lake Āraišu, Lake Trikātas and Teiči Bog, and the Lipari obsidian standard glass beam size obtained by electron probe microanalyses (EPMA).

Sample ID	SiO_2	TiO_2	Al_2O_3	FeO	MnO	MgO	CaO	Na_2O	K_2O	P_2O_5	Total	-Cl-	-F-
Lake Āraišu #1	73.78	0.92	12.7	3.72	0.1	0.83	2.54	2.96	2.25	0.2	100	0.03	0
Lake Āraišu #2	75.25	0.86	12.34	3.23	0.13	0.73	2.4	3.11	2.29	0.14	100.48	0.04	0.02
Lake Āraišu #3	74.93	0.86	12.47	3.88	0.11	0.75	2.59	3.35	2.35	0.18	101.48	0.04	0
Lake Āraišu #4	76.24	0.76	12.19	3.15	0.1	0.65	2.2	3.55	2.29	0.13	101.26	0.04	0
Lake Āraišu #5	76.22	0.82	12.58	3.45	0.17	0.66	2.33	2.96	2.24	0.18	101.61	0.03	0.18
Lake Āraišu #6	76.35	0.7	12.24	3.05	0.08	0.59	2.14	3.09	2.44	0.14	100.81	0.02	0
Lake Āraišu #7	77.75	0.7	12.48	2.88	0.1	0.6	2.16	2.99	2.42	0.14	102.22	0.03	0
Lake Āraišu #8	74.24	0.81	12.35	3.59	0.13	0.76	2.67	3.24	2.36	0.2	100.35	0.04	0.03
Lake Āraišu #9	73.38	0.83	12.57	3.87	0.11	0.77	2.91	3	2.08	0.19	99.72	0.05	0.03
Lake Āraišu #10	75.89	0.75	12.2	3.21	0.13	0.67	2.29	3.1	2.3	0.16	100.71	0.03	0.08
Lake Āraišu #11	74.26	0.79	12.12	3.3	0.11	0.72	2.5	3.13	2.31	0.14	99.39	0.03	0
Lake Āraišu #12	75.88	0.73	12.1	2.83	0.11	0.53	2.05	3.15	2.3	0.1	99.79	0.03	0
Lipari Obsidian													
20 µm-beam	74.64	0.1	12.55	1.43	0.05	0.05	0.75	3.89	4.85	0	98.32	0.34	0.06
15 µm-beam	75.06	0.06	12.75	1.46	0.08	0.03	0.7	4	5.09	0	99.24	0.34	0
10 µm-beam	75.07	0.11	12.75	1.45	0.06	0.02	0.74	4.02	4.87	0	99.1	0.36	0.07
Lake Trikātas #1	73.03	0.83	12.71	3.73	0.13	0.74	2.5	3.12	2.38	0.18	99.35	0.03	0
Lake Trikātas #2	72.5	0.87	12.81	3.87	0.05	0.77	2.72	3.38	2.31	0.23	99.5	0.04	0
Lake Trikātas #3	73.65	0.77	12.73	3.4	0.09	0.76	2.65	3.01	2.4	0.2	99.65	0.04	0
Lake Trikātas #4	71.98	0.86	12.79	3.82	0.1	0.77	2.7	2.88	2.31	0.11	98.35	0.04	0
Lake Trikātas #5	69.55	0.99	12.84	4.52	0.09	0.97	3.25	2.61	2.18	0.21	97.2	0.05	0
Lake Trikātas #6	70.98	0.85	12.79	3.87	0.11	0.79	2.74	2.85	2.38	0.15	97.52	0.02	0.05
Lake Trikātas #7	72.21	0.83	12.63	3.54	0.09	0.75	2.53	3.03	2.34	0.14	98.1	0.05	0
Lake Trikātas #8	74.93	0.73	12.54	2.94	0.16	0.52	1.95	2.94	2.55	0.08	99.35	0.04	0
Lipari Obsidian													
20 µm-beam	73.61	0.07	13.1	1.61	0.1	0.03	0.72	3.93	5.07	0.06	98.29	0.36	0
15 µm-beam	73.9	0.06	12.96	1.55	0.06	0.04	0.73	3.97	5.27	0.01	98.54	0.36	0
10 µm-beam	73.95	0.08	12.94	1.62	0.06	0.03	0.72	3.93	5.25	0	98.58	0.37	0
5 µm-beam	73.99	0.08	13.03	1.6	0.12	0.04	0.71	3.67	5.18	0.02	98.44	0.36	0
Bog Teiči #1	73.45	0.84	12.73	3.83	0.09	0.8	2.63	3.59	2.4	0.21	100.57	0.05	0
Bog Teiči #2	74.21	0.82	12.8	3.75	0.12	0.75	2.53	3.31	2.45	0.17	100.9	0.03	0
Bog Teiči #3	74.67	0.8	12.86	3.67	0.11	0.73	2.31	3.02	2.61	0.13	100.91	0.06	0
Bog Teiči #4	74.04	0.82	12.54	3.63	0.11	0.74	2.36	3.69	2.5	0.13	100.56	0.05	0
Bog Teiči #5	71.17	0.76	12.38	3.25	0.1	0.58	2.16	3.62	2.57	0.08	96.67	0.04	0.02
Bog Teiči #6	72.98	0.9	12.92	4.01	0.14	0.79	2.67	3.59	2.38	0.19	100.57	0.05	0
Bog Teiči #7	73.56	0.81	12.96	3.8	0.13	0.76	2.52	3.14	2.46	0.21	100.34	0.04	0
Lipari Obsidian													
20 µm-beam	73.64	0.06	13.22	1.6	0.09	0.04	0.73	3.88	5.11	0	98.37	0.35	0.01
15 µm-beam	73.68	0.06	13.13	1.66	0.02	0.01	0.71	3.82	5.37	0	98.46	0.35	0
10 µm-beam	74.87	0.08	13.16	1.53	0.07	0.05	0.72	3.9	5.11	0	99.49	0.36	0.05